

Emulsion Ripening through Molecular Exchange at Droplet Contacts

Kevin Roger,* Ulf Olsson, Ralf Schweins, and Bernard Cabane

Abstract: Two coarsening mechanisms of emulsions are well established: droplet coalescence (fusion of two droplets) and Ostwald ripening (molecular exchange through the continuous phase). Here a third mechanism is identified, contact ripening, which operates through molecular exchange upon droplets collisions. A contrast manipulated small-angle neutron scattering experiment was performed to isolate contact ripening from coalescence and Ostwald ripening. A kinetic study was conducted, using dynamic light scattering and monodisperse nanoemulsions, to obtain the exchange key parameters. Decreasing the concentration or adding ionic repulsions between droplets hinders contact ripening by decreasing the collision frequency. Using long surfactant chains and well-hydrated heads inhibits contact ripening by hindering fluctuations in the film. Contact ripening can be controlled by these parameters, which is essential for both emulsion formulation and delivery of hydrophobic ingredients.

Oil and water are immiscible fluids but they can still be “mixed” on the colloidal length scale, by forming droplets of one into the other. The resulting systems, emulsions, are intrinsically unstable and spontaneously evolve with time. Two mechanisms are known for the coarsening of an emulsion: droplet fusion (coalescence) and molecular exchange through the continuous phase (Ostwald ripening).^[1] The availability of these mechanisms determines the kinetics of the coarsening and it is thus widely believed that if both coalescence and Ostwald ripening are blocked, then emulsions are trapped in a metastable state.

However, rapid coarsening of emulsions has been observed under conditions where both coalescence and Ostwald ripening are strongly hindered. For instance, emulsions of hydrocarbon oils that are poorly soluble in water and protected by very strong monolayers of non-ionic surfactants, have been reported to coarsen rapidly.^[2–6] This observation led to the proposition that there was another mechanism for the exchange of oil molecules between droplets, which would

take place during collisions, through the exchange of oil molecules across the droplet–droplet interface.^[2,3,5]

If such a mechanism exists, it has serious consequences on the various uses of emulsions, both for industrial and academic purposes. Indeed, the existing formulation tools to hinder coalescence, by using surfactant layers of high preferred curvature,^[7,8] and Ostwald ripening, by trapping a poorly water-soluble specie in the droplet,^[9] may then fail to ensure any control of the emulsion metastability and structure. On the brighter side, identifying this mechanism would lead to a better understanding and thus better control of emulsions as delivery vectors. An abundant literature exists for applications where emulsions must deliver molecules to cells or microorganisms, a key issue in food and pharmaceutical industries.^[10,11] As these drug molecules are becoming more and more hydrophobic over the years, a pathway that does not require solubilization in an aqueous phase is of outstanding importance for delivery purposes. A mechanism of transfer by collisions between oil droplets and cells has been suggested based on global kinetic experiments.^[12]

Here we demonstrate that such a transfer mechanism exists and can in fact dominate the coarsening for emulsions stabilized by non-ionic surfactants. We use a recently developed method to produce monodisperse nanoemulsions in which all the surfactant is used at interfaces of the droplets, and none is left over as “free” surfactant micelles in the continuous phase.^[13,14] This avoids the possibility that oil molecules could be extracted from one droplet by a colliding micelle, transported inside that micelle, and delivered to the surface of another emulsion droplet.^[15] Moreover, the very small size of the droplets (initial radius 10 nm) prevents deformation of the droplet surfaces as they collide. Finally, this very small size also prevents gravity-induced separation (creaming) of the largest droplets as the coarsening progresses. All the nanoemulsions had the same composition: 1 % oil, 1 % polyoxyethylene alkyl ether ($C_{12}E_6$) surfactant, 98 % water. The properties of this class of surfactant are regulated by temperature, which controls the hydration of the hydrophilic head.^[1] At temperatures lower than the phase inversion temperature of the system, emulsions are expected to be protected against coalescence.^[7,8]

We examine two types of exchange: 1) exchange of identical oil molecules between droplets of slightly different sizes, driven by the reduction of total interfacial area (size-driven) and 2) exchange of different oil molecules between droplets of identical sizes, driven by the mixing entropy of the oils (composition-driven).

We measured the variation with time of the droplets mean volume using dynamic light scattering and cumulant analysis, since the autocorrelation function exhibits a single decay. Panel A of Figure 1 displays the variation of the mean volume growth rate of the droplets, $d(\frac{4}{3}\pi R_{\text{mean}}^3)/dt$, as a function of the

[*] Dr. K. Roger

CNRS, Laboratoire de Génie Chimique
31030 Toulouse (France)

E-mail: kevin.roger@ensiacet.fr

Dr. K. Roger, Prof. Dr. U. Olsson
Division of Physical Chemistry, Chemical Center
Lund University, 22100 Lund (Sweden)

Dr. R. Schweins
DS/LSS Group, Institute Laue-Langevin
6 Rue Jules Horowitz, 38042 Grenoble Cedex 9 (France)

Dr. B. Cabane
CBI, CNRS, ESPCI
10 rue Vauquelin, 75231 Paris Cedex 05 (France)

Supporting information for this article is available on the WWW under <http://dx.doi.org/10.1002/ange.201407858>.

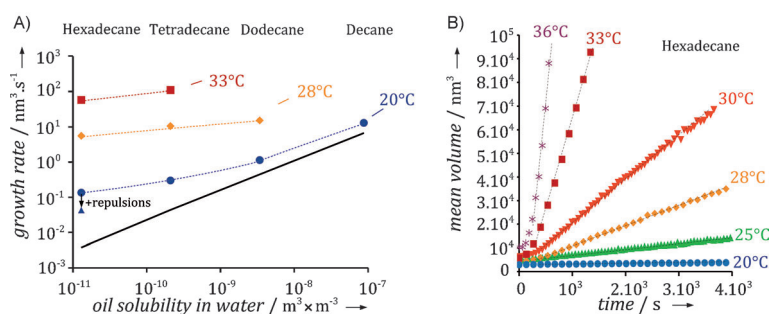


Figure 1. A) Volume growth rate of nanoemulsions stabilized by C_{12}E_5 surfactant as a function of oil solubility in water and temperature. At the lowest temperature, the prediction from the LSW theory of Ostwald ripening (black line) is in agreement with the measured rates for the shorter oils but not for the longer ones. This deviation dramatically increases with the rise of the temperature. B) Growth of the mean droplet volume with time for a hexadecane/ C_{12}E_5 nanoemulsion at various temperatures. The volume growth rate is extracted as the slope of the linear variation with time after a short lag phase.

oil solubility in water, for three temperatures. The black line corresponds to the theoretical rates, nearly independent of the temperature in the observed range, calculated from the Lifshitz–Slyozov–Wagner (LSW) theory corrected by the concentration of the droplets (see the Supporting Information). At 20°C, the experimental rates are consistent with theory for the most soluble oils (decane, dodecane), but deviate for the less soluble oils (tetradecane, hexadecane). At higher temperatures, the deviation between experimental and theoretical rates increases by orders of magnitude: Ostwald ripening is not the coarsening mechanism. We are thus monitoring an exchange process between oil droplets that does not take place through the continuous aqueous phase but through direct contacts between droplets. To confirm this, we added 4% of sodium octylsulfate anionic surfactant in the interfacial film of the droplets (with no impact on their size). This resulted in a decrease of the growth rate, as shown in Figure 1 (see also the Supporting Information). Therefore, preventing droplet contact through long-range repulsions indeed slows down this exchange mechanism. An additional argument in favor of a contact mechanism is the rapid increase of the growth rate with the droplet concentration (see Supporting Information), which is inconsistent with the weak concentration dependence of Ostwald ripening.^[16] The set of growth curves for the poorly water-soluble hexadecane oil is displayed in panel B of Figure 1 as a function of temperature. The growth rate increases by orders of magnitude with the temperature, and thus with the surfactant hydration, which also shows the importance of the surfactant film and points towards a contact process (see the Supporting Information). We obtained similar results with other types of emulsions with larger mean diameters and polydispersities.

We now turn towards demonstrating that this coarsening mechanism is not droplet coalescence, although it operates upon droplet contact. Distinguishing two mechanisms operating at contact through a size distribution analysis is difficult. Instead, we used a method that consists in tracking the oils originating from different droplets. We added a highly

efficient exchange drive, which is the mixing entropy of different oils. To ensure that the mechanism remained unchanged we used oils of identical physicochemical properties, except for their neutron scattering length densities. We designed a contrast-manipulated small-angle neutron scattering (SANS) experiment, in which the contrast between droplets and bulk is easily tuned by selective deuteration. This experiment was performed on the D11 instrument at ILL.^[17]

We prepared two nanoemulsions of identical chemical composition but different isotopic composition: the first one was made of normal hexadecane, $\text{C}_{16}\text{H}_{34}$, and the second one of perdeuterated hexadecane, $\text{C}_{16}\text{D}_{34}$. Both were made in the same bulk aqueous phase, which was a mixture of H_2O and D_2O (0.585/0.415 volume fractions) that nearly matches the scattering length density of a droplet composed of a 1–1 mixture of $\text{C}_{16}\text{H}_{34}/\text{C}_{16}\text{D}_{34}$ covered by pentaerythritol dodecyl ether (C_{12}E_5). In the scheme presented in panel A of Figure 2, the

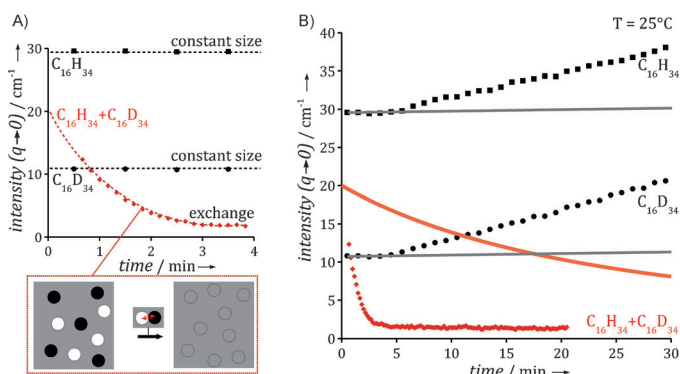


Figure 2. Contrast manipulated small-angle neutron scattering (SANS) experiment. Parent emulsions scattered intensities are displayed as black squares ($\text{C}_{16}\text{H}_{34}$) (“black droplets”) and black circles ($\text{C}_{16}\text{D}_{34}$) (“white droplets”). The scattered intensity of the 1:1 mixture of these two parent emulsions is displayed as red diamonds. The continuous phase is a $\text{H}_2\text{O}/\text{D}_2\text{O}$ mixture that nearly matches the scattering length density of the 1:1 mixture of the two oils, leading to zero contrast if the droplets exchange molecules. Panel A displays the first few minutes of the experiment: the scattered intensity of the 1:1 mixture collapsed to a plateau value, which means full exchange took place, while the scattered intensities of the parent emulsions, thus their droplets sizes, remained constant, which means coalescence did not occur. This exchange is also much faster than the prediction from a composition-driven Ostwald ripening mechanism (orange line). At longer times, displayed on panel B, the parent emulsions scattered intensities rise slowly and linearly due to the reduction of interfacial area, with the same rate as displayed on Figure 1.

first emulsion was made of black droplets ($\text{C}_{16}\text{H}_{34}$) in a gray solvent ($\text{H}_2\text{O}/\text{D}_2\text{O}$), and the second of white droplets ($\text{C}_{16}\text{D}_{34}$) in the same gray solvent. The two “parent” emulsions were then mixed, so that if the droplets exchanged molecules we would then obtain gray droplets in a gray solvent, resulting in a collapse of the scattering contrast and thus of the scattered intensity.

Figure 2 displays the scattered intensities, extrapolated at low scattering vector magnitude q , of “parent” emulsions ($C_{16}H_{34}$ black squares and $C_{16}D_{34}$ black circles) and the 1:1 mixture of the two (red diamonds). Panel A displays the first minutes of the exchange. The “parent” emulsions yielded a constant scattered intensity, in the ratio of their contrast with the bulk, which directly means that the droplet size was constant over that time range. This lag time was also observed in our dynamic light scattering measurements as seen on Figure 1 and corresponded to an increase of the polydispersity of the population. Strikingly, the intensity of the 1:1 mixture of the two emulsions collapsed to a very low value during this lag time. This implies that the contrast of the droplets of the mixed emulsion vanished within a few minutes, and thus that they had fully exchanged their oils. Since this exchange took place at constant droplet sizes we can rule out coalescence as the exchange mechanism. Panel B shows that at much longer time, the intensity of the “parent” emulsions slowly increases and thus that the droplets grew through uneven exchange of oil molecules. The growth rate was identical to the one deduced from previous dynamic light scattering measurements displayed on Figure 1.

This set of data also confirms that an Ostwald ripening mechanism cannot account for the observations. Indeed, the theoretical rates corresponding to droplets exchanging their oil molecules through the continuous aqueous phase do not match the experimental rates, whether for composition-driven (compare orange line to red symbols in Figure 2) or size-driven (compare gray lines to black symbols in Figure 2) Ostwald ripening (full calculation in the Supporting Information).

We now turn towards the microscopic mechanism through which oil molecules are exchanged between droplets at contact. Figure 3 displays three pathways. Pathway I consists in the non-correlated permeation of oil molecules across an unperturbed bilayer;^[3] the transport rate is determined by the crossing of the two hydrophilic layers, in which the oil solubility is very low. Pathway II corresponds to the opening of transient channels in the surfactant films allowing several oil molecules to go through;^[2] since we are far from the phase inversion temperature, the spontaneous curvatures of the

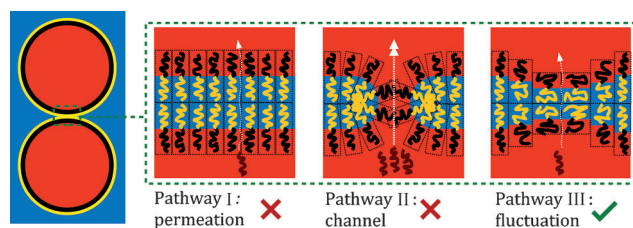


Figure 3. Three microscopic pathways for contact ripening. Pathway I consists in the non-correlated permeation of oil molecules across an unperturbed bilayer. Pathway II corresponds to the opening of large channels in the surfactant films allowing several oil molecules to go through. Pathway III corresponds to a synchronous decrease in the thickness of both hydrophilic and hydrophobic surfactant layers, with a correlated increase in the area per surfactant molecule. The resulting local thinning and disordering of the surfactant layer favors the oil transfer between droplets. Only pathway III is consistent with the data from Figure 4.

surfactant films are high and the hole growth is controlled by the two bending constants κ and $\bar{\kappa}$.^[7,8] Pathway III results from a synchronous decrease in the thickness of both hydrophilic and hydrophobic surfactant layers, with a correlated increase in the area per surfactant molecule.

These pathways will be differently impacted by increasing the surfactant hydrophilic and hydrophobic chains. We thus prepared similar nanoemulsions with two series of pure surfactant homologs. The first corresponds to an increase of the hydrophilic chain length, $C_{12}E_5$, $C_{12}E_6$, $C_{12}E_7$. The second corresponds to an increase of the hydrophobic chain length, $C_{12}E_6$, $C_{14}E_6$, $C_{16}E_6$. The results are displayed on Figure 4 and show that increasing either the hydrophilic or the hydrophobic chain length results in a decrease by orders of magnitude of the contact ripening rate.

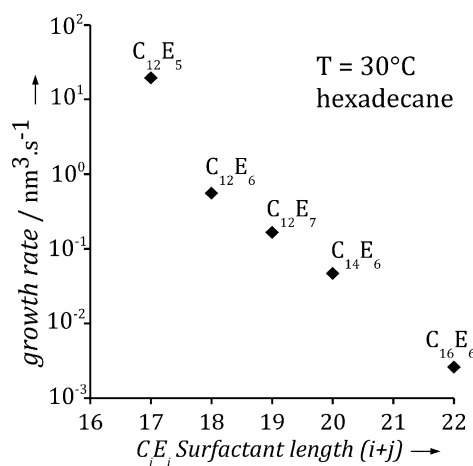


Figure 4. Growth rates for similar emulsions prepared with two series of surfactant homologs, $C_{12}E_5$, $C_{12}E_6$, $C_{12}E_7$ and $C_{12}E_6$, $C_{14}E_6$, $C_{16}E_6$. The growth rate decreases by orders of magnitude with increasing either the hydrophobic chain or the hydrophilic head. This corresponds to the hindrance of density fluctuations in the surfactant layers when using longer amphiphilic molecules.

The influence of the hydrophobic chain length is inconsistent with pathway I, which is only limited by the hydrophilic layer. The symmetrical influence of both hydrophilic and hydrophobic chain length on the exchange rate is also inconsistent with pathway II since the bending constants only weakly depend on the chain length and in an asymmetrical manner: increasing the hydrophobic chain length results in a weak increase of κ while increasing the hydrophilic chain length results in a weak decrease of $\bar{\kappa}$.^[18] Also this pathway is incompatible with the strong increase of the ripening rate with the temperature, although the system is much below its phase inversion temperature.^[7] Only pathway III is consistent with the data from Figure 4 as local fluctuations in the area per surfactant molecule will be hindered by increasing both hydrophobic and hydrophilic chain length.

To conclude, we have demonstrated that even if both coalescence and Ostwald ripening are blocked, another mechanism, contact ripening, may allow molecular exchange between emulsion droplets. Two types of parameters control the contact ripening rate: those that control the surfactant

layer structure, such as its hydration and cohesiveness, and those that control the probability of collisions, such as the concentration of droplets and long-range repulsions. Exposing this previously hidden pathway brings an array of opportunities: if the desired application requires to store the emulsion in a metastable state, we can now make sure all the exchange pathways are efficiently blocked, while if emulsions are used as delivery carriers we can now improve the transfer.

Received: August 1, 2014

Revised: October 8, 2014

Published online: December 10, 2014

Keywords: coarsening · colloids · emulsions · exchange · small-angle neutron scattering

-
- [1] F. D. Evans, H. Wennerström, *The Colloidal Domain: Where Physics, Chemistry, Biology, and Technology Meet (Advances in Interfacial Engineering)*, Wiley-VCH, Weinheim, **1999**.
- [2] V. Schmitt, C. Catelet, F. Leal-Calderon, *Langmuir* **2004**, *20*, 46. PMID: 15744998.
- [3] L. Taisne, *Echanges d'huile entre gouttes d'emulsions*, Ph.D. thesis, Paris 6, **1997**.
- [4] L. Taisne, P. Walstra, B. Cabane, *J. Colloid Interface Sci.* **1996**, *184*, 378.
- [5] A. Evilevitch, *Molecular exchange in colloidal dispersions*, Ph.D. thesis, Lund University, **2001**.
- [6] O. Sonnevile, *Mousses biliquides*, Ph.D. thesis, Paris 6, **1997**.
- [7] A. Kabalnov, H. Wennerström, *Langmuir* **1996**, *12*, 276.
- [8] A. Kabalnov, J. Weers, *Langmuir* **1996**, *12*, 1931.
- [9] A. J. Webster, M. E. Cates, *Langmuir* **1998**, *14*, 2068.
- [10] D. McClements, E. Decker, J. Weiss, *J. Food Sci.* **2007**, *72*, R109.
- [11] *Pharmaceutical Emulsions and Suspensions* (Eds.: F. Nielloud, G. Marti-Mestres), Marcel Dekker, New York, **2000**.
- [12] D. Decker, S. Vroegop, T. Goodman, T. Peterson, S. Buxser, *Chem. Phys. Lipids* **1995**, *76*, 7.
- [13] K. Roger, B. Cabane, U. Olsson, *Langmuir* **2010**, *26*, 3860. PMID: 19899785.
- [14] K. Roger, U. Olsson, M. Zackrisson-Oskolkova, P. Lindner, B. Cabane, *Langmuir* **2011**, *27*, 10447.
- [15] J. Weiss, C. Cancelliere, D. J. McClements, *Langmuir* **2000**, *16*, 6833.
- [16] A. Brailsford, P. Wynblatt, *Acta Metall.* **1979**, *27*, 489.
- [17] P. Lindner, R. Schweins, *Neutron News* **2010**, *21*, 15.
- [18] T. Sottmann, R. Strey, *J. Chem. Phys.* **1997**, *106*, 8606.
-